

Alma Mater Studiorum - University of Bologna

**RHS Footpeg for a Supersport Bike in Additive
Manufacturing Aluminium**

a project for Chassis and Body Design and Manufacturing

Professor:

Massimiliano De
Agostinis

Student:

Zappalorti Luca

Table of Contents

1. Assignment	3
2. Material and manufacturing process	3
A Material	3
B Manufacturing Process	4
3. 2D Structural analysis	5
A General hypothesis	5
B Brake leverage scheme	6
C Footpeg holder scheme	6
4. FEM simulation: from validation to optimization	7
A 3D CAD Model	7
B ANSYS® Static Structural Analysis (model validation)	8
C ANSYS® Topological Optimization	9
5. FEM simulations: from reverse engineering to model check	10
A CAD Model reverse engineering	10
B Final model Static Structural Analysis	11
C Threaded joints validation (Static Structural) on REV10	11
6. Printing Preview	12

1. Assignment

The object of the study is the right footpeg holder from Ducati Street Fighter V4 S. It is hold in position by two threaded joints; moreover, the holder is coupled to the footpeg through a hinge and linked to the brake lever and to the brake pump supports.

Therefore, its job is to hold the rider, the brake pedal and the brake pump.

The goal to be achieved is to redesign the footpeg holder using the additive manufacturing technic, modelling the holder trough a FEM topological optimization. Specifically, it is necessary to reach a footpeg tip displacement between -6 mm and -8 mm respect to the vertical direction, using an aluminium alloy.

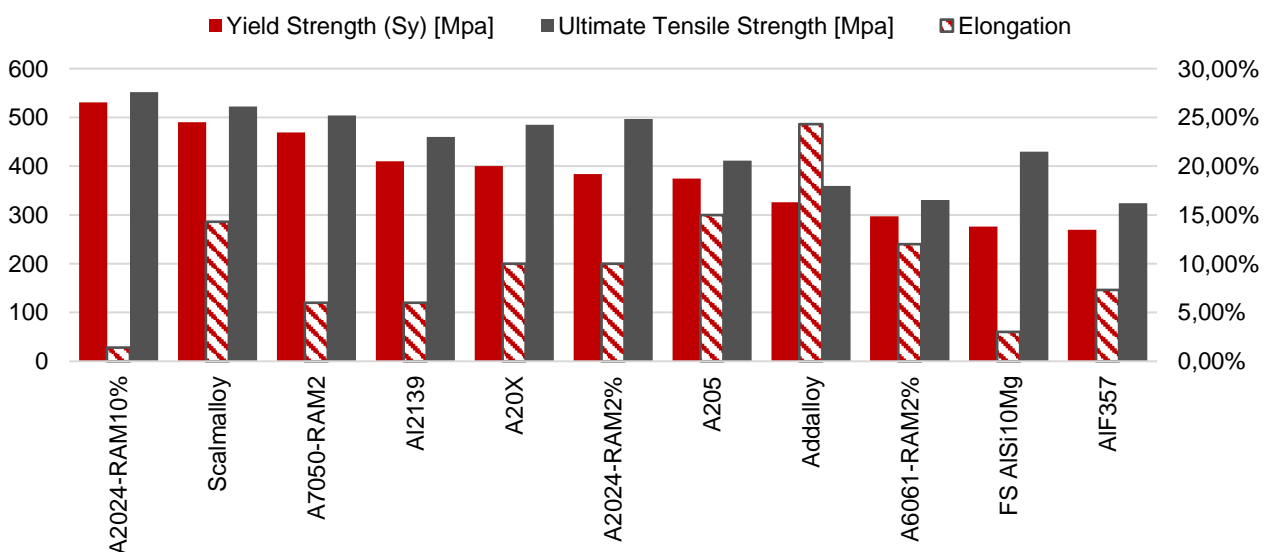
2. Material and manufacturing process

A Material

The material assigned is an Aluminium AM alloy. After research in Total Materia database, it has been identified the top ten alloys in terms of Yield Strength. In the following table and chart there is a comparison among these alloys, which is based on the Yield strength (Sy), the Ultimate Tensile Strength (UTS) and elongation at break (E%)

Material Designation	A2024-RAM10%	Scalmalloy	A7050-RAM2	Al2139	A20X	A2024-RAM2%	A205	Addalloy	A6061-RAM2%	FS AISi10Mg
Yield Strength [Mpa]	531	490	469	409,95	400	384	375	326	297	276
Ultimate Tensile Strength [Mpa]	552	522,5	504	460	485	497	411,5	359,5	331	430
Elongation	1,4%	14,3%	6,0%	6,0%	10,0%	10,0%	15,0%	24,3%	12,0%	3,0%

Table 1 - Top ten AM aluminium alloys by Sy [Source: Total Materia]



Graph 1 - Top ten AM aluminium alloys mechanical properties comparison [Source: Total Materia]

As shown in Graph 1, has been chosen *Scalmalloy*® because it is the best trade-off among all materials available in terms of mechanical properties, although is quite expensive (cost is not a design requirement). *Scalmalloy*® is the commercial name of Aluminium–Magnesium–Scandium alloy patented by APWORKS for additive manufacturing, so it is currently used in aerospace, motorsport, automotive and robotics.

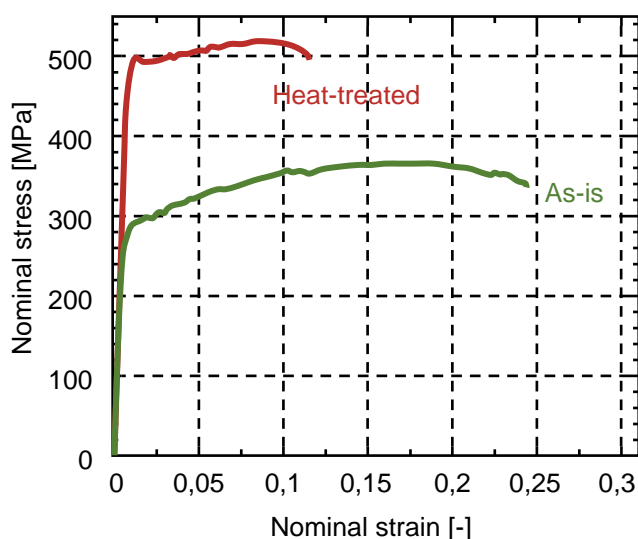
In the following tables and graphs there is a review of the main mechanical properties of this alloy:

Element	Mg	Sc	Zr	Mn	Si	Fe	Zn	Cu	Ti	O	V
Wt%	(min)	4.00	0.60	0.20	0.30	0.00	0.00	0.00	0.00	0.00	0.00
	(max)	4.90	0.80	0.50	0.80	0.40	0.40	0.25	0.10	0.015	0.05

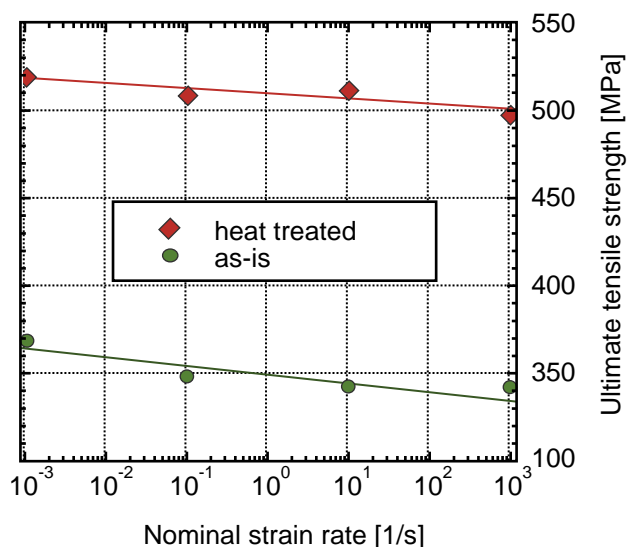
Table 2 – Mean chemical composition of *Scalmalloy* [Source: APWORKS]

Yield Strength (Sy)	470 MPa
Ultimate Tensile Strength (UTS)	520 MPa
Elongation at break (E%)	13%
Young's Modulus	70 GPa
Density	2,67 kg/dm ³
Vickers Hardness	180 HV
Supply Conditions	Heat treated and machined
Manufacturer	AIRBUS APWORKS GmbH
Price	4'000 – 6'000 €/Kg

Table 3 – *Scalmalloy*® main properties [Source: APWORKS]



Graph 2 - Tensile tests results (heat-treated vs as-is) [Source: APWORKS]



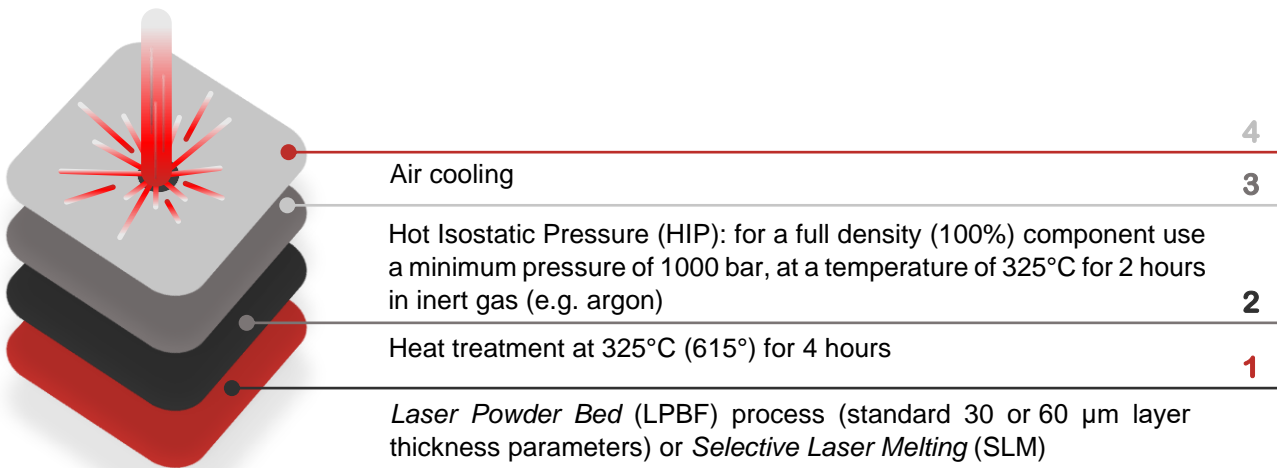
Graph 3 - Ultimate tensile strength on strain rate (heat-treated vs as-is) [Source: APWORKS]

The material has excellent mechanical properties, which combined with the low density makes it perfect for the manufacturing of lightened and corrosion resistant components with high ductility.

B Manufacturing Process

Additive manufacturing is a process that allows to produce components starting directly from the 3D file designed using cad software. So, it is possible to produce, coat and repair components with very high performances and design freedom. Indeed, thanks to a layer-by-layer production, unlike to the machined processes which are instead subtractive, it is possible to realize complex geometry, like the holder.

The full manufacturing process is composed of:



Due to the high cooling rates and rapid solidification, a unique microstructure is achieved: coupling the material properties with the design freedom provided by AM processes we can obtain high performance parts, previously impossible to achieve.

3. 2D Structural analysis

A General hypothesis

As a first step, a two-dimension scheme of the structure was made in order to determine the loads and constrain reaction: these data are necessary for the model validation.

The initial specifications are:

- A vertical load F_{z1} of 1500N applied 15 mm from the end of the footpeg;
- A vertical load F_{z2} of 500 N acting on the centreline of the brake pedal.

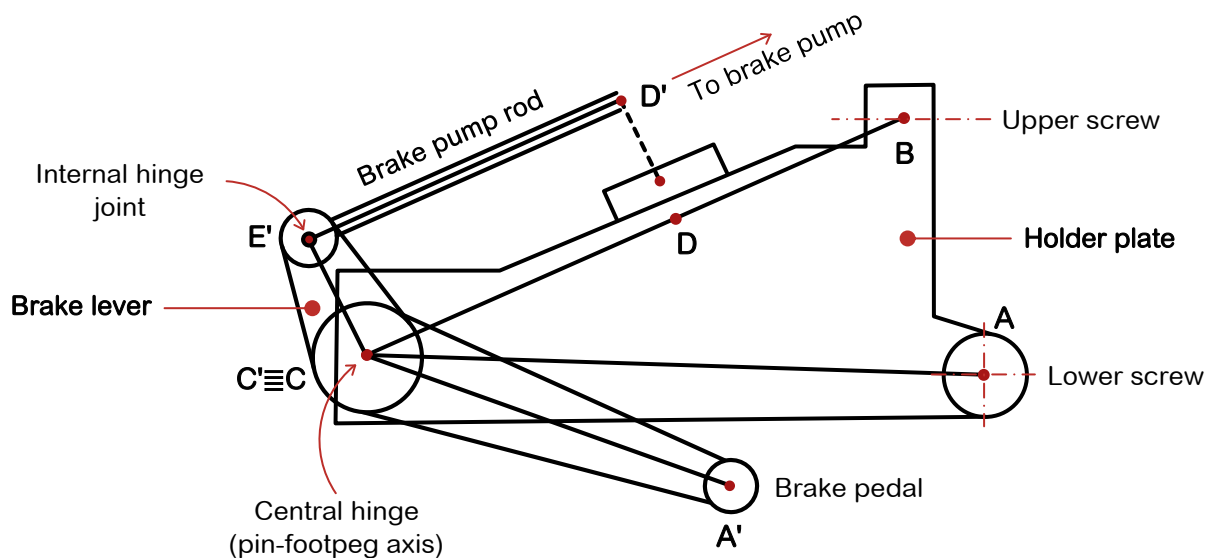


Figure 1 - Total 2D structural scheme

Additional geometric and mechanical assumptions are required to obtain the two-dimensional model.

- Plate and brake lever developed in the plane;
- All loads are acting in the identified plane;
- No bending moment derived from F_{z1} and F_{z2} transportations in the transversal direction;

- Brake pedal at end stop;
- The holder is understood as a V-shaped beam;
- The brake leverage is developed as a system of rods;
- The pump mounts are schematised as one.

As a first consideration, the model was divided into two sub-structures: brake system structure and holder structure. In this way it is possible to study the two systems separately and get the reactions they exchange.

B Brake leverage scheme

In the original model, the brake pump lever is coupled to the pump rod with an internal hinge and it is supposed, as an engineering choice, that the brake lever is hinged at the axis of the footpeg. In the simplified one an internal hinge is introduced to model the joint coupling the brake pump rod and the brake lever. A second hinge is shaped to replace the brake lever pivot (coaxial with the footpeg) and a third hinge is used to represent the two brake pump cylindrical supports, attached to the footpeg holder.

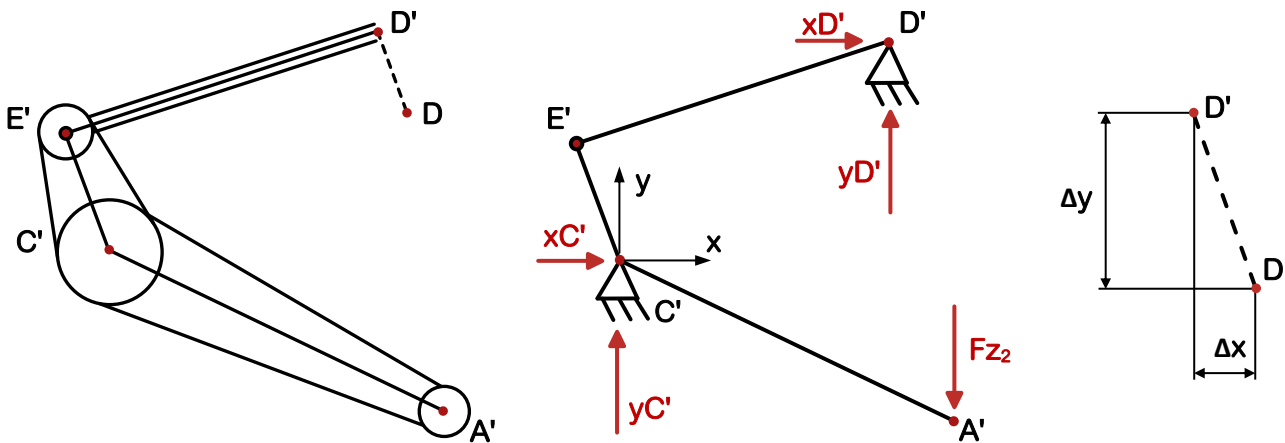


Figure 2 - Brake leverage structural scheme

By solving the isostatic structure, the following constraint reactions are obtained, which can then be transferred to the model of the holder

$x_{C'}$	1270 N	$x_{D'}$	-1270 N
$y_{C'}$	875 N	$y_{D'}$	-375 N

Table 4 - Brake leverage reactions results

Reporting the constraining reactions on the holder structure, it is necessary to consider that the forces applied at point D' must be translated at point D (Figure 2), so transport moments are therefore necessary:

$$M_{tot} = x_{D'} \cdot \Delta y + y_{D'} \cdot \Delta x = 39,757 \text{ Nm}$$

C Footpeg holder scheme

The footpeg holder scheme consist of one "V"- shaped beam element and it is loaded as follows:

- f_{z1} is applied in C;
- $x_{C'}$ and $y_{C'}$ (previously computed) acts on point C;
- Break pump reactions are applied on D, also taking into account the transport moment.

Solving the hyperstatic structure, the following constrains reaction are obtained:

x_A	2707 N	y_B	-2707 N
y_A	844 N	y_B	156 N

Then this reaction must be compared with those obtained from the FEM simulation to validate the simulation model.

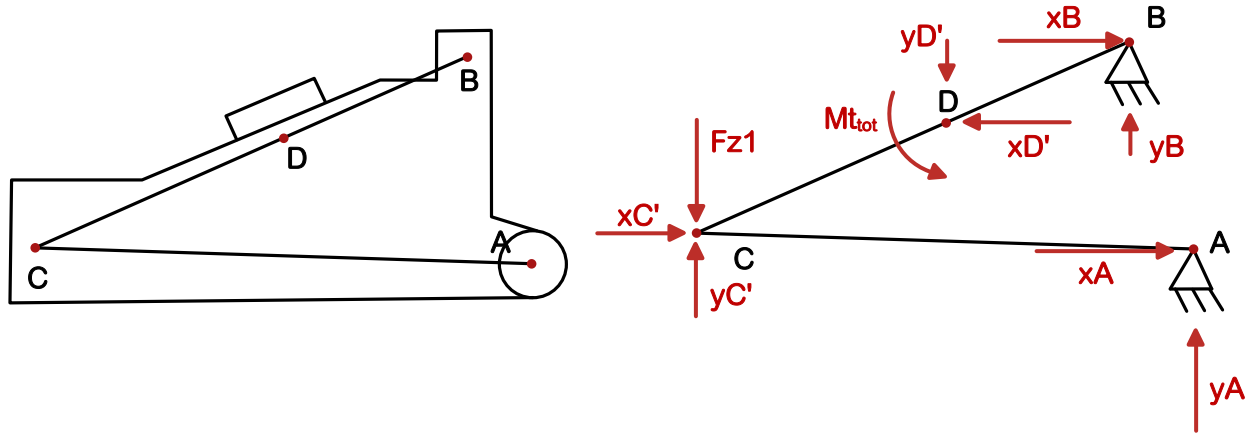


Figure 3 - Footpeg holder structural scheme

4. FEM simulation: from validation to optimization

A 3D CAD Model

To construct the FEM model and validate it, it is necessary to start from a 3D CAD geometry that takes account of:

- Previous assumptions [3.A General hypothesis];
- Geometric references imposed as initial constraints (screws position, footpeg position, brake lever position);
- Geometric boundaries condition (fairing volumes);
- Footpeg to be assumed as “rigid” for displacement calculations;
- No permanent deformation allowed upon unloading;
- The surplus material needed to make topological optimiser works, necessary not to exclude a priori solution;
- The commercial solution.

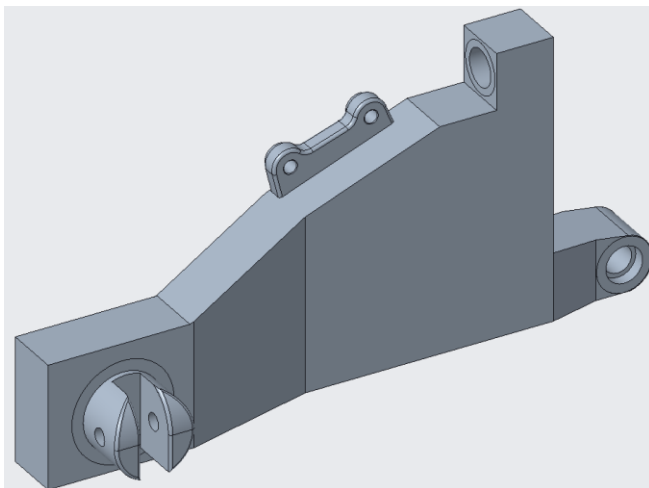


Figure 5 - 3D CAD model for validation

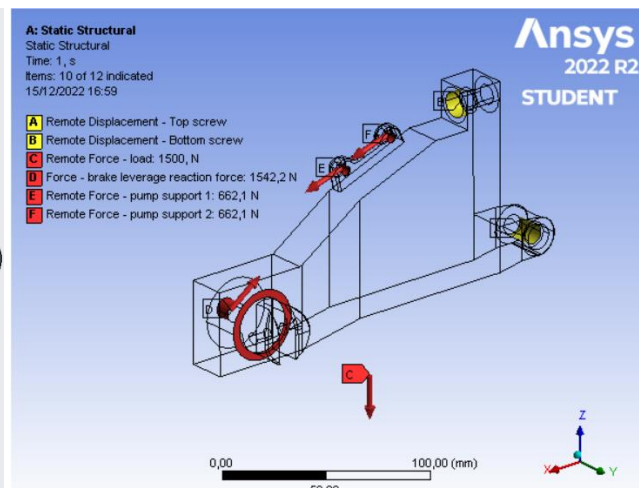


Figure 4 - FEM validation model set-up in ANSYS®

B ANSYS® Static Structural Analysis (model validation)¹

Geometry

The model identified so far was used for the validation of the geometry itself.

Coordinate systems and remote points

To correctly locate the point of application of the force Fz1, it is useful to introduce a local coordinate system at the axis of the footpeg.

A remote point is introduced to set the footpeg force attached to the nodes of the footpeg holder attachment face, with this is possible to simulate the force acting on the footpeg by the rider without designing the footpeg itself (point C in Figure 4);

Mesh

Mesh was first set to 5 mm size in the entire body, with adaptive sizing. Then it was made a convergence study reducing step by step the mesh size until 4 mm with a 1.2 mesh growth rate and no capture curvature or proximity;

Static structural analysis

The static structural analysis carried out is a single step analysis with a time interval [0,1] s.

To report a force on the model, it is necessary to use the *remote force* command of ANSYS®, which allows to create a rigid constraint between the point of application of the force and the mesh nodes of the surface to which the force is associated.

The input forces were the assignment load Fz1 and the brake lever reactions obtained from the B.Brake leverage scheme. I.e., to apply Fz1 the *remote force* command needs the remote point selection. The footpeg holder force (-1500 N) was acting on the Z axis (according with the global coordinate system shown in Figure 4) at 15 mm away from the footpeg holder external side, while the brake force was acting on the other side of the footpeg holder hinge with components -1270 N (X axis) and 875 N (Z axis). The constraining reaction of the brake pump, which is 1270 N (X axis) and 375 N (Z axis), has been set splitting the load into two footpeg supports.

In addition, the action of the screw was modelled without designing them using remote displacement constraints acting on their hole (all translation and rotational movements are suppressed except for the rotation through each screw axis). The remote displacement command behaves in the same way as the remote force command, i.e., it creates a rigidly constrained application point with the nodes of the mesh of the constraint surface.

Results

It was asked to the software to process the following data as output:

- a) Z axis directional deformation [mm];
- b) Total deformation [mm];
- c) Equivalent (Von-Mises) stress [MPa];
- d) Reaction forces in correspondence of top and bottom screws (remote displacements) [N];
- e) Footpeg tip (remote point) Z axis displacement [mm].
- f) For the validation of the model only the constraint reactions on the screw are necessary.

In Table 5, there is a comparison between the analytical reaction forces calculated in correspondence of hinge constraints in 2D model and the numerical reaction forces obtained from the remote displacements of ANSYS® analysis. Since they had the same order of magnitude and even close values, it is possible to consider the model verified and continue with the developing of the structural model.

¹ See the attached Warped_REV.wbpj file

Results		Analytical	Warped_REV.wbpj	
			FEM	e%
Upper Screw Reaction [N]	X	2707	2,584.30	-4.53%
	Y	- ²	-1,791.90	-
	Z	156	176.10	12.88%
Lower Screw Reaction [N]	X	-2707	-2,854.30	5.44%
	Y	-	1,791.90	-
	Z	844	823.89	-2.38%
Footpeg Tip Displacement (Remote Point) [mm]		-0.04064	-0.77299	1802.04% ³

Table 5 - Comparison among analytical and validation results

C ANSYS® Topological Optimization

As a first step, previous structural simulation results were used as input for topological optimization, it follows that these two analyses share the same assumptions and constraints.

Optimization Region

The entire body of the holder was set as the optimization zone, while the screw connections, the pump support flange and the holder's region of attachment to the footpeg were set as the exclusion zone.

Objective

The simulation objective was to maximize the stiffness (or minimize the compliance) of the model.

Response Constraints

At this point, two types of response constraint have been set: mass, retained from 100 % to 50 % and finally to 18%, and remote point (point C in Figure 4 - FEM validation model set-up in

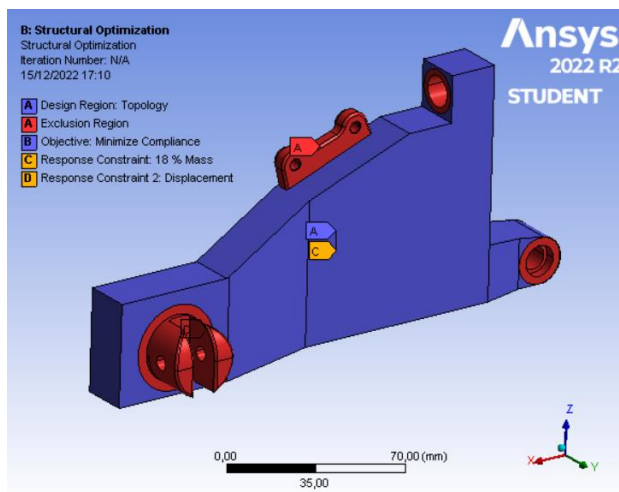


Figure 7 - Structural optimization set-up

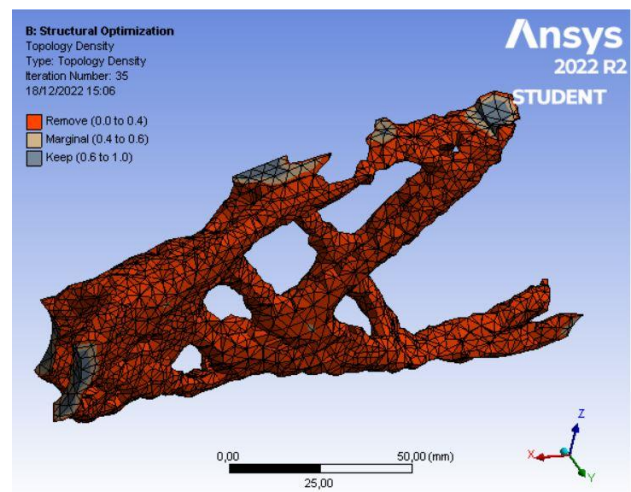


Figure 6 - Optimized mesh

ANSYS® Figure 4) Z axis displacement up to -8 mm.

² Reactions in the y-direction cannot be determined using the simplified 2D model in 3.A General as they are due to the bending stress components

³ The error in the displacement is again due to the bending components neglected in the simplifications of the two-dimensional model

Results

At the end of the simulation, we got an optimized structure in which the software removed all the zones where stresses were low, based on its specific response constraints and objective.

As the percentage of retained mass decreases, the software removes more and more material in the inner body of the plate to get a proper box structure, which is better able to withstand torsional and bending moment stresses. As a final consideration, output mesh file shows some cut off sub-structures due to the removal of material. In order to get a proper mesh structure, it is required to modify the mass retain threshold to restore part of the material.

5. FEM simulations: from reverse engineering to model check

A CAD Model reverse engineering

The engineering reconstruction of the part obtained from the structural optimization simulation was imported as a mesh (STL) into the CAD software as a shadow to redesign the part. An iterative process of CAD software reverse engineering reconstruction and static structural simulations (with the previous constraints) was then followed, focusing on the reduction of equivalent stresses of Von-Mises and increasing footpeg tip displacement until the reaching of the requirements assigned. Table 6 shows all the steps followed and the results got in terms of screw reactions, footpeg tip displacement and max equivalent stress (von-Mises).

Results		REV1	REV2	REV3	REV4	REV5	REV6	REV7	REV8	REV9	REV10
Upper Screw Reaction [N]	X	1882	2156	2174	2176	2174	1918	2202	2199	1925	-2195
	Y	-1618	-1574	-1572	-1558	-1558	-1592	-1543	-1533	-1531	-1530
	Z	1027	1431	1420	1426	1427	893	1176	1174	1157	1165
Lower Screw Reaction [N]	X	-1882	-2155	-2174	-2176	2174	1918	2203	2199	2185	2195
	Y	1618	1574	1571	1558	1557	-1592	1534,3	1533,2	1531,2	1530,3
	Z	-401,5	-431,1	-420,3	-426,6	-426,8	-267,6	-176	-174	-157	-166
Footpeg Tip Displacement [mm]		-2,980	-3,947	-4,30	-5,86	-6,17	-7,300	-7,726	-7,398	-6,799	-6,569
Max Equivalent Stress [MPa]		634	1246	986	1775	1773	1297	1021	826	688	722

Table 6 - Reverse model iterations: once the displacement goal was achieved, further iterations were necessary to minimise concentrated stresses (plasticised zones)

The topological optimization has reduced the weight of the holder from its initial weight of 0,685 kg to 0,240 kg: engineering reconstruction has returned a final component of 0,182 kg.

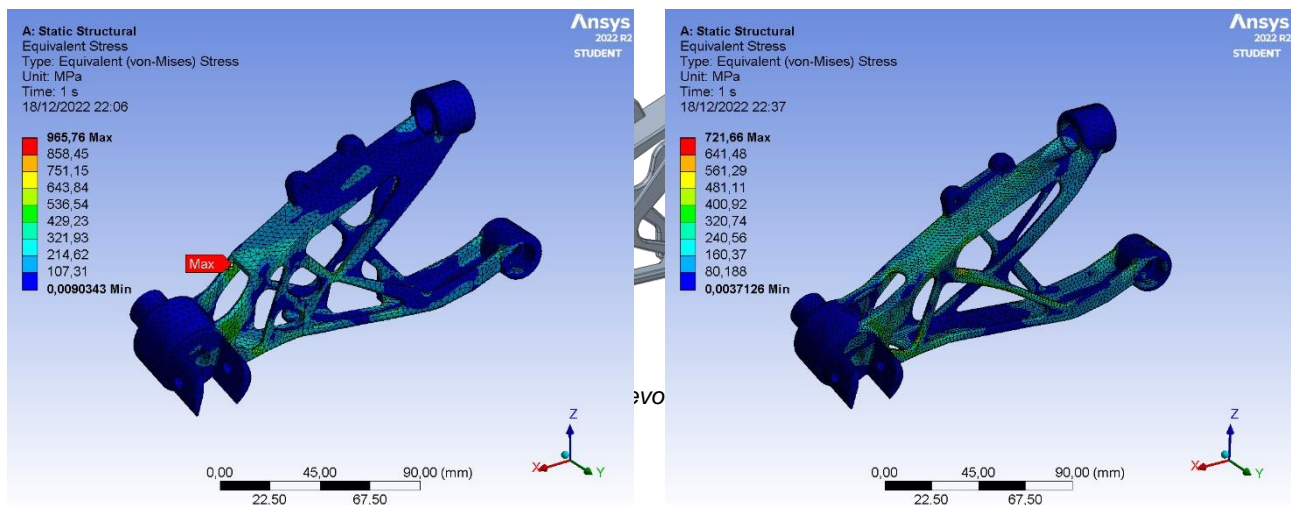


Figure 9 - Equivalent Stress comparison: REV10 [right] has less extensive stress concentrations than REV 6 [left]

B Final model Static Structural Analysis

To validate the final model, a new structural analysis is performed, which incorporates the constraints of the previous analyses. The entire structure is low-stressed, apart from a few areas that are beyond the yield strength and failure limit. This is because these areas are subjected to mesh defects, and therefore subjected to computational approximations. Indeed, it is possible to appreciate how individual mesh element shows a huge growth up to 300 MPa equivalent stress.

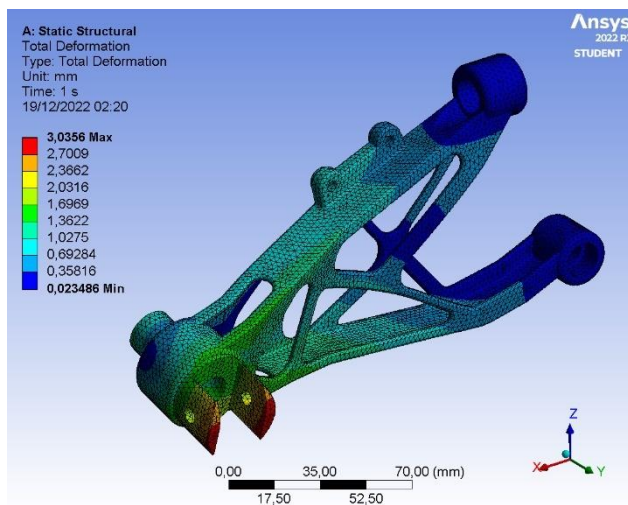


Figure 11 - REV10 Total Deformation distribution

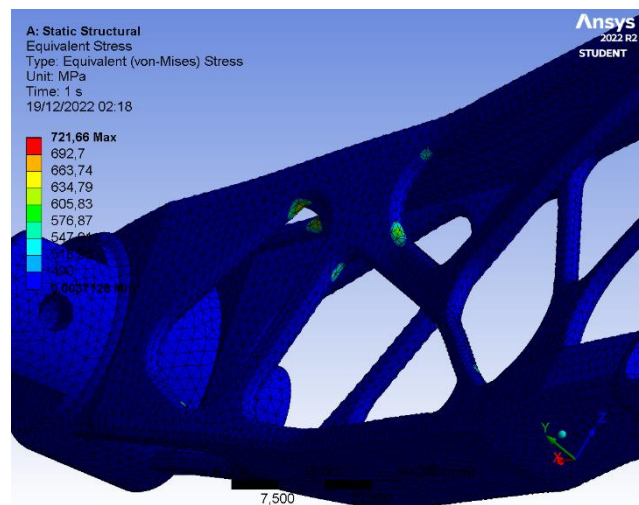


Figure 10 - REV10: detail of stress concentrations

C Threaded joints validation (Static Structural) on REV10

The threaded joints design was performed according to the data provided by international standard EN ISO 898 - 1. It was supposed to use class 8.8 M-profile screws, considering a stress factor of 1.3 and a safety coefficient of 3. As a first step, the reaction forces in each screw hole (remote displacement constraint) were extracted from the first static structural simulation; therefore, the calculation of the minimum stress area [mm²] was done by multiplying the stress factor [-] for the safety coefficient [-] and for the axial force [N] and dividing all by the stress proof load [N/mm²] of the screw, so a screw with an equal or greater stress area was chosen.

Based on the previous screw choice, the suggested axial preload [N] and tightening torque [Nm] were identified from VDI 2230 guideline. Following this approach, M8x1 screw were chosen for both

the footpeg attachments to the frame and M5x0.5 screw for both the brake pump supports. Moreover, an assembly preload of 17 kN and a tightening torque of 41.2 Nm were found for the first couple of screws.

The last static structural analysis is a multi-step analysis with a time interval [0,2] s divided into two equally spaced sub-steps [0,1] - [1,2] s with a program controlled auto time stepping: its target is to validate the screw design that has been performed before.

From the previous static structural simulations, some constraints have been recycled and some have been replaced with others. In particular, remote displacement constraints were replaced with a pair of M8x1 screws coupling the holder with the motorbike frame, which is modelled as two separated parallelepiped boxes with a nut in each one. Moreover, a bolt pretension acting on the shank of each screw has been set in the first time substep [0,1] s. In the last substep are instead set the assignment forces and the brake lever reactions.

In this case, an automatic search of contact regions was established between the three bodies and then an additional fixed support was set on the external face of each box.

As in the previous static structural simulation, the mesh was first set to 5 mm size in the entire body, with adaptive sizing and then a convergence study was carried out reducing the size until 3 mm with 1.4 growth rate and no capture curvature or proximity.

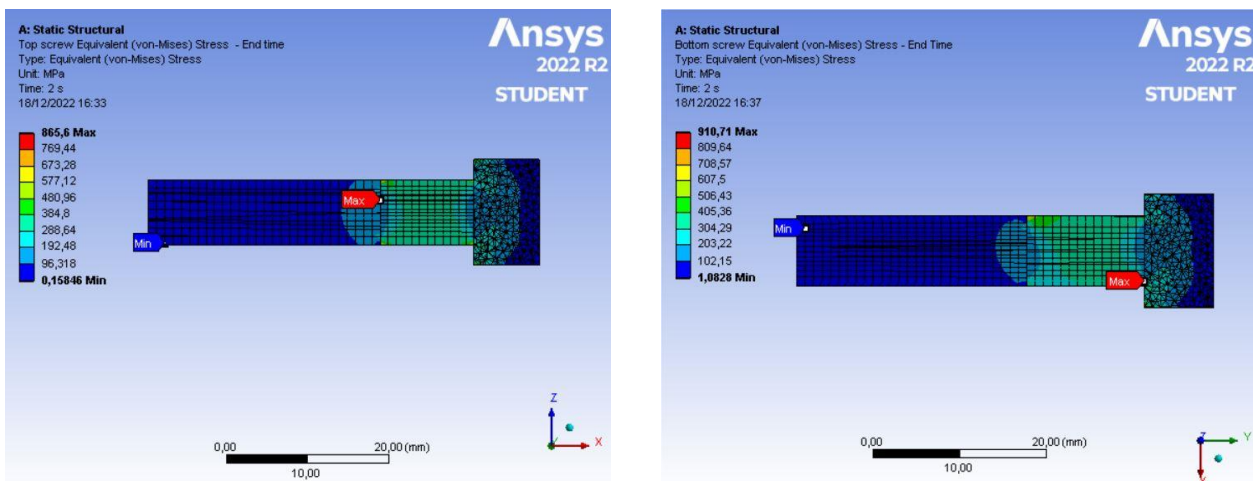
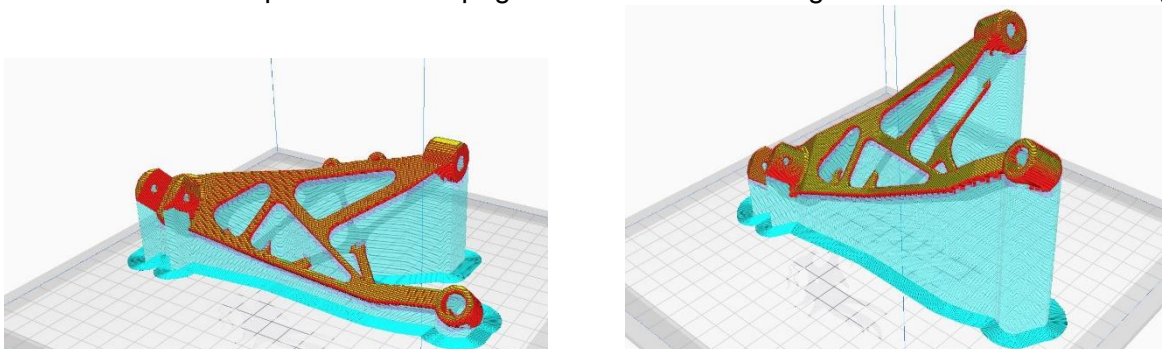


Figure 12 - Screws equivalent stress distribution

The outputs required were equivalent Von-Mises stress [MPa] on both the screws coupling the holder with the motorbike frame. Evaluating the stresses distribution on Figure 12, obtained by a section plane cutting each screw into two bodies through their axis, the screw design was validated neglecting small stress concentrations at the boundary interfaces.

6. Printing Preview

At the end of design phase, it was performed a printing preview of the final component, which could be manufactured in at least two different ways of relative positioning plate-supports, in order to evaluate which is the best solution in terms of printing time, material cost and surfaces roughness. First one is rotated respect to the footpeg X axis and has the target to increase surface roughness



of footpeg body without spending too much time in printing and money in supports; while the second one is rotated respect to the footpeg X and Y axis to realize better quality screw holes.